CONF-8504305--1

UCRL--92902

DE87 009587

AN EXPERIMENT TO MEASURE THE ELECTRON NEUTRINO MASS USING A CRYOGENIC TRITIUM SOURCE

O. Fackler, B. Jeziorski, W. Kolos, H. Monkhorst,
M. Mugge, H. Sticker, K. Szalewicz, R. M. White
R. Woerner

This Paper was prepared for submittal to the
Rencontres de Moriond Conference on Weak
Interactions, Les Arcs, France - April, 1985

June 25, 1985

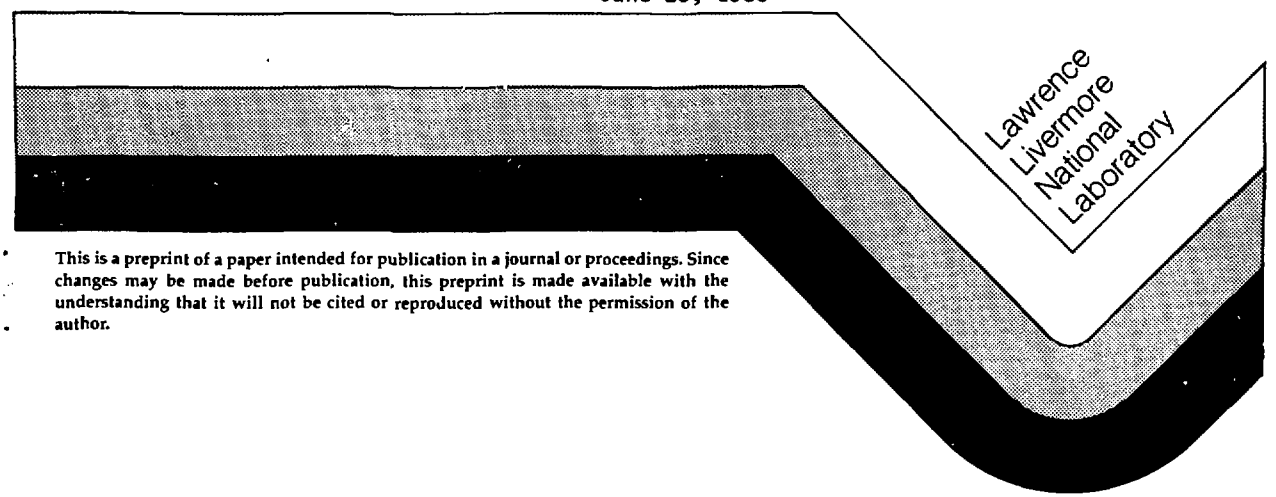

AN EXPERIMENT TO MEASURE THE ELECTRON NEUTRINO MASS USING A CRYOGENIC TRITIUM SOURCE

O. Fackler[‡,*], B. Jeziorski[‡,**], W. Kolos[‡,+], H. Monkhorst[*], M. Mugge[†,‡], H. Sticker[*], K. Szalewicz[‡,+], R. M. White[‡], R. Woerner[‡]

‡ Lawrence Livermore National Laboratory
Livermore, CA 94550
* Rockefeller University
New York, NY 10021
** University of Warsaw, Warsaw, Poland
** University of Waterloo, Waterloo, Ontario, Canada
+ University of Florida, Gainesville, Florida 32611
† Fermilab, Batavia, IL 60510

ABSTRACT

We are performing an experiment to determine the electron neutrino mass with the precision of a few eV by measuring the tritium beta decay energy distribution near the endpoint. Key features of the experiment are a 2 eV resolution electrostatic spectrometer and a high-activity frozen tritium source. It is important that the source have electronic wavefunctions which can be accurately calculated. These calculations have been made for tritium and the HeT^+ daughter ion and allow determination of branching fractions to 0.1% and energy of the excited states to 0.1 eV. We discuss the excited final molecular state calculations and describe the experimental apparatus.

The goal of our experiment is to measure the neutrino mass to better than 2 eV. If the neutrino mass is finite, the tritium beta decay energy distribution changes appreciably only within a few neutrino masses from the endpoint (see Fig. 1). For a zero neutrino mass, the fraction of decays within 2 eV of the endpoint is only 2.6×10^{-12}. This small fraction dictates a low-background, high-resolution spectrometer with large acceptance. After beta decay, the resulting atom or molecule can be left in one of many excited states. These excited states take energy from the emerging beta and give rise to a number of branches, each with a different endpoint energy, in the beta energy distribution. The sum of these branches results in the observed Kurie plot. An accurate physics result emerges only if one knows the occupation fractions and energies of these final excited states and hence, the expected shape of the measured distribution. In addition, the spectrometer resolution function must be well understood. A wide resolution function or long tails in this function can introduce a significant smearing in the tritium beta decay spectrum. Such effects greatly complicate the interpretation of the data. Finally, the emerging electrons undergo a dE/dx loss in the source itself. Ideally, a measurement of the dE/dx loss is made and a consistant neutrino mass is determined in sources of different thicknesses.

For complex molecules or tritium binding processes, the final state effects are not calculable with sufficient precision for a high accuracy measurement. However, molecular tritium (T_2) at liquid helium temperatures is ideal because the low intermolecular binding energy (on the order of 1/400 eV) means it essentially has the electronic wavefunction of the free T_2 molecule.

We have calculated the β-decay energy spectrum which results from the decay of one of the nuclei in the T_2 molecule[1,2]. An accurate, explicitly correlated basis set was used to describe the electronic states of both the parent and daughter molecules. All channels which meaningfully effect the spectrum have been incorporated in the calculation including the resonance and scattering channels.

Unlike the atom, the HeT^+ ion in its ground state has both vibrational and rotational degrees of freedom which can absorb energy from the decay beta. At the liquid helium temperature of our source, only the lowest vibrational and rotational states are populated. However, after the decay, when one of the atoms has been given an impulse from the decay beta, most of the possible vibrational and rotational states will be populated for transitions to bound states. The details of these calculations will be presented in Ref. 3.

These calculations have been performed independently by another group[4] using totally different techniques. In particular, the electronic wavefunctions were

determined using a complete configuration interaction calculation. In all cases the agreement between these approaches was exceedingly good.

The HeT^+ is primarily excited to a high vibrational state when, near the endpoint of the beta decay distribution, the decay beta is emitted nearly aligned with the internuclear axis. Conversely, the HeT^+ ion is left in a highly excited rotational state when the decay beta is emitted nearly perpendicular to the internuclear axis. This coupling between the beta decay and the vibrational and rotational states gives a high density of states near the top of the potential well (see Fig. 2). The full width at half height of this distribution is about 0.7 eV. As a consequence of this small spread, the ground state branch in the Kurie plot is smeared by only an average of 1 eV. This additional spread is a small penalty to pay for the ease of using molecular rather than atomic tritium.

We present the results of our calculations in the form of a Kurie Plot. These plots have been generated using the formula

$$K(\varepsilon;m_\nu) = \sum_n \left| P_n K^2(\varepsilon;E_n,m_\nu) \right|^{1/2}$$

where ε is the energy measured relative to the endpoint of the spectrum, m_ν is the neutrino mass, E_n is the energy level, and P_n is the transition probability to this level. The energy E_n is measured with respect to the lowest energy value in a given treatment of nuclear motion. If the electronic spectrum of the daughter ion is used, this lowest energy value is its ground state energy for the T_2 equilibrium nuclear distance, ($R = 1.4$ bohr), or its ground state energy averaged over the ground vibration of the initial T_2 system. If the nuclear-motion-resolved calculations are used, E_n is relative to the ground rovibronic level of $^3HeT^+$. $K(\varepsilon;E_n,m_\nu)$ is a single branch of the Kurie plot defined as

$$K(\varepsilon;E_n,m_\nu) = (m_\nu + \varepsilon - E_n)^{1/2} \left[(m_\nu + \varepsilon - E_n)^2 - m_\nu^2\right]^{1/4}$$

for $\varepsilon \geq E_n$, and $K(\varepsilon;E_n,m_\nu) = 0$ for $\varepsilon < E_n$. For the continuous part of the spectrum, the summation is changed to an integration.

In Fig. 3 we compare Kurie plots obtained for pure nuclear, atomic, and molecular (T_2) tritium decay processes for an assumed 30 eV neutrino mass. The molecular plots are presented for three cases: (1) constructed for a fixed internuclear distance ($R = 1.4$ bohr); (2) obtained for R averaged over the ground state vibration of the T_2 molecule; (3) same as (2) except for a complete treatment of the final state nuclear motion for

the most significantly contributing $^3HeT^+$ electronic states. The final result of this work is presented in plot (3).

Fig. 3 clearly shows that the Kurie plot is comparably effected far from the endpoint by final state effects in both the atom and the molecule. However within about 3 eV from the endpoint the molecular rovibrational effects are much more important than the atomic effects. This distortion is only about 3 eV and is accurately calculated.

The Kurie plots resulting from this calculation are presented for neutrino masses between 0 and 50 eV in Fig. 1. The plots become practically linear above 100 eV and are very close to linear for $\epsilon > 75$ eV.

Strictly speaking, these results only apply to gaseous T_2. Our source is actually solid tritium rather than a free molecule. Nevertheless, the tritium molecular wavefunction in the frozen solid is very close to the molecular wavefunction of the free molecule. We can understand this qualitatively by noting that the tritium melting temperature implies that the intermolecular binding energy is very much less than the orbital electron binding energy. Consequently we can expect a very small pertubation on the molecular wavefunction because of intermolecular binding forces. Quantitively, the electron probability density halfway to the nearest molecular neighbor is approximately 2×10^{-4} of the maximum. This small electronic overlap gives rise to a negligible distortion of the molecular wavefunction. The depth of the internuclear potential well is approximately 1,600 times that of the intermolecular potential well. This difference in binding energies also indicates a very small pertubation of the molecular wavefunction in the solid.

The experimental evidence for a very small change in the electronic wavefunctinn resulting from the binding in the solid comes from Raman spectra in gaseous and solid hydrogen. The vibrational energy levels are determined by the shape of the internuclear potential well and the shape of this well is determined by the electronic wavefunction. The typical measured shift in the vibrational energy levels resulting from the binding in solid hydrogen is about 1/2000 eV. Since this energy shift is very small compared with the typical vibrational energy level spacing of about 0.1 eV, this is evidence for a very small perturbation in the molecular wavefunctions resulting from the intermolecular binding in the solid. Furthermore, the molecular binding forces are so weak that the rotational states are hardly perturbed and the molecules can rotate as though they were nearly free. We conclude that the fractional change in the wavefunction due to intermolecular binding in the solid is less than 0.1%. Hence our results apply to both gaseous and frozen T_2.

The experimental apparatus is shown in Figure 4. It is contained in a vacuum tank 0.9 m in diameter and 7 m long. The tank is passively shielded by 2 concentric

magnetic shields giving a residual field of less than 2 milligauss in the active region. The source is a liquid helium cooled plate on which tritium is frozen. Varying the amount of tritium gas introduced allows source thickness variation from a few monolayers up to any thickness. The source points upstream allowing the decay electrons to enter a region which is the electrostatic analog of a parabola with the source at its focus. Hence, electrons emerging from the source are mapped into a larger essentially parallel beam traveling downstream.

Following the electrostatic parabola, a variable-length collimator defines the angular acceptance of the electrons and limits the maximum angle which the electrons can make with the axis of the electrostatic spectrometer. The spectrometer consists of three equally spaced grid planes with field shaping electrodes around the axis. We measure the integral number of electrons within the passband of the electrostatic parabola whose energies are higher than the center grid potential. Electrons leaving the spectrometer pass through an electrostatic lens which focusses them onto a solid state detector. This detector simply counts the electrons but does have an energy resolution of approximately 1.5 keV which aids in rejecting low energy electrons and photons.

The experimental apparatus was tested by looking at the 7.3 keV electron conversion electrons from ^{57}Co. This line has an intrinsic HWHM of 0.6 eV. Our measurement of this line showed a HWHM of 2 eV. This measured distribution is shown in Figure 5. The tail on the low energy side is due to the occurance of close-lying satellites of the conversion lines produced by accompanying shake-off excitations.

In conclusion, we have discussed why frozen tritium is an ideal source offering the highest activity per dE/dx of any material and offering fully calculable final state effects. These final state effects contribute less than 0.2 eV of uncertainty to the final possible determination of the neutrino mass. In addition, we have built a spectrometer with a measured resolution of better than 2 eV. Monte Carlo studies indicate that by using a frozen source our apparatus will be able to determine the neutrino mass to better than 2 eV.

1) W. Kolos, B. Jeziorski, K. Szalewicz, and H. J. Monkhorst, Phys. Rev. A31, 551 (1985).
2) W. Kolos, B. Jeziorski, H. J. Monkhorst, and K. Szalewicz, Intern. J. Quantum Chem. S19, 000 (1985).
3) B. Jeziorski, W. Kolos, K. Szalewicz, O. Fackler, and H. J. Monkhorst, Phys. Rev. A, submitted.
4) N. Winter and O. Fackler, Lawrence Livermore National Laboratory, unpublished.

Work performed under the auspices of the U.S. Department of Energy by the Lawrence Livermore National Laboratory under contract No. W-7405-ENG-48, by FermiLab and by Rockefeller University.

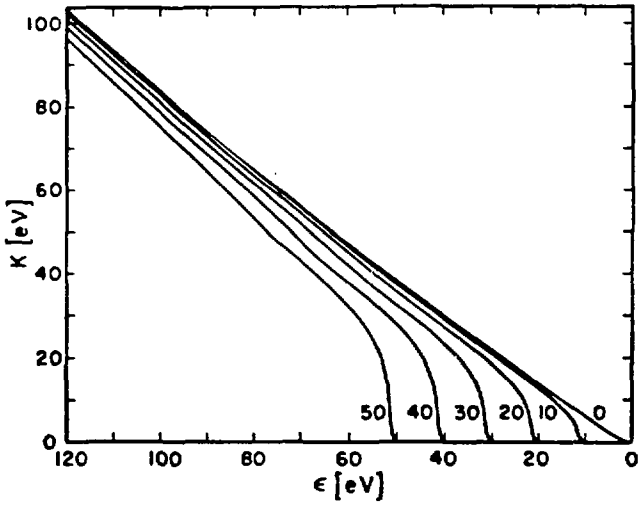

Fig. 1. Kurie plots for m_ν = 0 (10) 50 eV

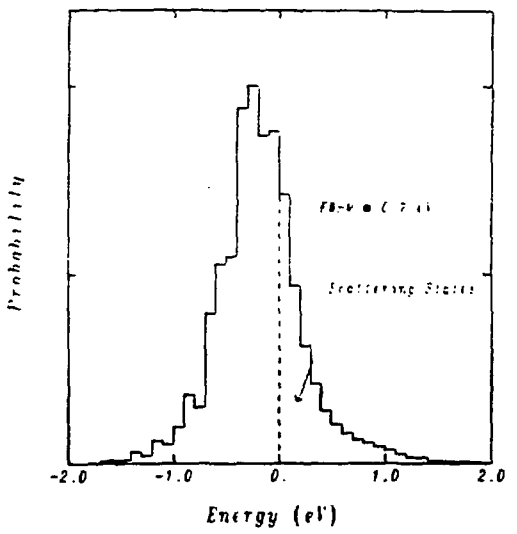

Fig. 2. Energy Spread Introduced by Molecular Vibration and Rotation

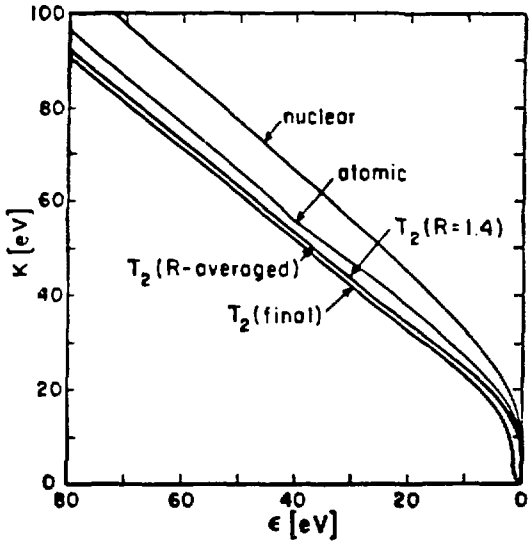

Fig. 3. Kurie Plots Assuming m = 30 eV

For 1) Nuclear decay

2) Atomic decay

3) T_2 decay with R_i = 1.4 Bohr

4) T_2 decay averaged over initial molecular vibration

5) Same as 4) but including final state vibration and rotation

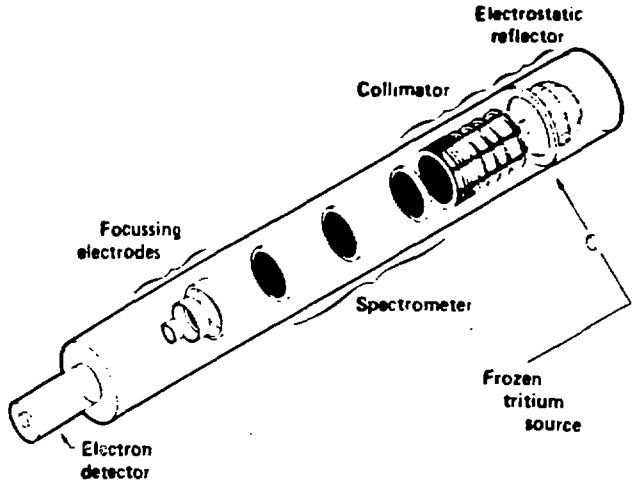

Fig. 4. Schematic Diagram of the Experimental Apparatus

- Measurements using ^{57}Co - source of monoenergetic electrons (E = 7.302 keV)
- Natural width of 7.302 keV line $\simeq$ 1.2 eV

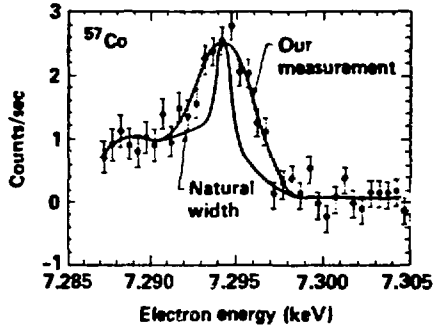

Measured HWHM is 2 eV = resolution < 2 eV

Figure 5 Measured Spectrometer Resolution. The Low Energy Tail is Due to "Shake Off" Effects